

COMPUTATIONAL SIMULATION OF A PLANE CHANNEL WITH $K - \varepsilon$ AND MULTI-DIRECT FORCING METHOD

Gabriel M. Magalhães

Faculty of Mechanical Engineering
Federal University of Uberlândia (UFU)
Av. João Naves de Ávila 2121, 38400-902
Uberlândia-MG, Brazil
gabrielmarcosmag@gmail.com

Jessica G. de Freitas Santos

Faculty of Mechanical Engineering
Federal University of Uberlândia (UFU)
Av. João Naves de Ávila 2121, 38400-902
Uberlândia-MG, Brazil
jessica.guarato@ufu.br

Marcelo M. R. Damasceno

Faculty of Mechanical Engineering
Federal University of Uberlândia (UFU)
Av. João Naves de Ávila 2121, 38400-902
Uberlândia-MG, Brazil
mdamasceno@ufu.br

João M. Vedovoto

Faculty of Mechanical Engineering
Federal University of Uberlândia (UFU)
Av. João Naves de Ávila 2121, 38400-902
Uberlândia-MG, Brazil
vedovoto@ufu.br

Aristeu da Silveira Neto

Faculty of Mechanical Engineering
Federal University of Uberlândia (UFU)
Av. João Naves de Ávila 2121, 38400-902
Uberlândia-MG, Brazil
aristeus@ufu.br

ABSTRACT

The computational simulation of flows with immersed bodies requires special treatments when cartesian grids are used. The treatment of the velocity field for flows with immersed bodies is the theme of several works found in the literature. However, for non-isothermal flows, turbulent flows, using Unsteady Reynolds Average Navier-Stokes (URANS) methodology, and scalar transport, it is necessary to consider the treatment for such transported properties along the immersed boundary. Several methodologies for representing immersed boundaries (IB) already exist. One of these methodologies is the Multi-Direct Forcing (MDF), which is approached in the present work. The IBM can be applied not only in simulations of flows around complex geometries but also in simulations of flows inside these geometries. Thus, the present work presents a proposal to treat the dissipation rate ε [m^3/s^2], when using a $k - \varepsilon$ model together with the MDF. The results are presented for a flat channel and for the flow around a cylinder, in which the responses for different characteristics of the flow are analyzed.

INTRODUCTION

The simulation of flows with immersed bodies using regular and cartesian meshes is the object of several works in literature, each one with a different proposal. These proposals have positive and negative aspects. The difficulty of

implementation, the accuracy of results and computational cost are different for each one. One possibility of working with immersed bodies is to use two separate meshes, an Eulerian mesh, and a Lagrangian mesh. The Eulerian mesh corresponds to the computational domain that resolves the fluid transport equations, and the Lagrangian mesh is used to represent the immersed body geometry. The Multi-Direct Forcing (MDF) proposed by Wang *et al.* (2008) is one example of an immersed boundary method (IBM). In the present work, the MDF is applied.

The objective of the MDF is to force the desired value of some information at the body boundary. For example, the velocity at the surface of a stationary sphere in a fluid flow is null, so the desired value of the velocity forced by the MDF at the sphere boundary is zero. Therefore, the MDF includes a source term in the Navier-Stokes equations associated with the forced value. This source term is obtained by the difference between the estimated value of information during the new time step, which is interpolated at the Lagrangian mesh points, and the forced value. So, as the source term is calculated in each Lagrangian mesh points, it has to be distributed to the nearest Eulerian mesh points. The interpolation and the distribution are performed using the hat function. Finally, this process is repeated in a loop. The use of the MDF method for velocity fields was studied by several authors, but there are few studies based on the MDF method associated with the Unsteady Reynolds Average Navier-Stokes (URANS) methodology.

This work presents a novel methodology for using the standard k - ε and MDF method with cartesian and non-cartesian geometries.

METHODOLOGY

For the present work, it was used the standard k - ε model, proposed by Launder & Spalding (1972) and, also the two-layer wall treatment model to simulate internal flows. The standard k - ε model requires two more transport equations besides the Navier-Stokes equations and the continuity equation.

The first equation of this model transports the turbulent kinetic energy, k [m^2/s^2], and it is given by

$$\frac{\partial(\rho k)}{\partial t} + \bar{u}_j \frac{\partial(\rho k)}{\partial x_j} = \frac{\partial}{\partial x_j} \left[\left(\mu + \frac{\mu_t}{\sigma_k} \right) \frac{\partial k}{\partial x_j} \right] + \mu_t S^2 - \rho \varepsilon, \quad (1)$$

where ρ is the specific mass of the fluid, μ and μ_t are the molecular and the turbulent dynamic viscosities, respectively, $\sigma_k = 1.0$ is a model constant and $S = \sqrt{S_{ij}S_{ij}}$, in which S_{ij} represents the strain rate tensor components.

For the MDF method, it is necessary to force a value for the turbulent kinetic energy at the body boundary. As the velocity at a wall is null, the boundary condition of the immersed boundary for the turbulent kinetic energy is also null.

The second equation transports the dissipation rate, ε [m^3/s^2], and it is given by

$$\frac{\partial(\rho \varepsilon)}{\partial t} + \bar{u}_j \frac{\partial(\rho \varepsilon)}{\partial x_j} = \frac{\partial}{\partial x_j} \left[\left(\mu + \frac{\mu_t}{\sigma_\varepsilon} \right) \frac{\partial \varepsilon}{\partial x_j} \right] + C_{\varepsilon 1} \frac{\varepsilon}{k} \mu_t S^2 - \rho C_{\varepsilon 2} \frac{\varepsilon^2}{k}, \quad (2)$$

where $\sigma_\varepsilon = 1.3$, $C_{\varepsilon 1} = 1.44$ e $C_{\varepsilon 2} = 1.92$ are the model constants.

The methodology for forcing k and ε

To deduce the methodology it is necessary to consider two transport equations for the property, in this case the turbulent kinetic energy, k .

The first transport equation is to estimated k , named k^* . It is the (1) for k^* , given by:

$$\frac{\partial(\rho k^*)}{\partial t} + \bar{u}_j \frac{\partial(\rho k^*)}{\partial x_j} = \frac{\partial}{\partial x_j} \left[\left(\mu + \frac{\mu_t}{\sigma_k} \right) \frac{\partial k^*}{\partial x_j} \right] + S_k, \quad (3)$$

where $S_k = \mu_t S^2 - \rho \varepsilon$.

The second equation is the Eq. (1) with a term f_k , which f_k is a term relative to MDF.

$$\frac{\partial(\rho k)}{\partial t} + \bar{u}_j \frac{\partial(\rho k)}{\partial x_j} = \frac{\partial}{\partial x_j} \left[\left(\mu + \frac{\mu_t}{\sigma_k} \right) \frac{\partial k}{\partial x_j} \right] + S_k + f_k, \quad (4)$$

Using the Euler method for discretization of the temporal term at Eq. (3) and (4) and includes a term equivalent

to zero in the Eq. (4):

$$\frac{\rho^{(n+1)}k^{(n+1)} - \rho^{(n-1)}k^{(n-1)}}{\Delta t} + \frac{\rho^{(n+1)}}{\Delta t} (k^{*(n+1)} - k^{*(n+1)}) + \bar{u}_j \frac{\partial(\rho k)}{\partial x_j} = \frac{\partial}{\partial x_j} \left[\left(\mu + \frac{\mu_t}{\sigma_k} \right) \frac{\partial k}{\partial x_j} \right] + S_k + f_k, \quad (5)$$

where ρ is the density of fluid.

Rearranging the Eq. (5) it is possible to obtain a system with two equations. The Eq. (6) is the transport equation for k and the Eq. (7) gives the source term of the MDF.

$$\frac{\rho^{(n+1)}k^{*(n+1)} - \rho^{(n-1)}k^{(n-1)}}{\Delta t} + \bar{u}_j \frac{\partial(\rho k)}{\partial x_j} = \frac{\partial}{\partial x_j} \left[\left(\mu + \frac{\mu_t}{\sigma_k} \right) \frac{\partial k}{\partial x_j} \right] + S_k, \quad (6)$$

$$f_k = \frac{\rho^{(n+1)}}{\Delta t} (k^{(n+1)} - k^{*(n+1)}). \quad (7)$$

The first step in the MDF is to interpolate the values of k^* to the Lagrangian point, obtaining the value of k^* in each Lagrangian point, $k^*(L)$. After the interpolation, it is possible to calculate the Lagrangian force $F_{k(L)}$ with the equation:

$$F_{k(L)} = \frac{\rho^{(n+1)}}{\Delta t} (k_{(L)}^{(n+1)} - k_{(L)}^{*(n+1)}), \quad (8)$$

where $k_{(L)}^{(n+1)}$ is a correct value of the property at immersed boundary.

After the calculus of $F_{k(L)}$ it is necessary to distribute this value to Eulerian points with the same scheme was used in the interpolation obtaining $f_{k(E)}$. This value is used for calculating $k_{(E)}^{(n+1)}$ with the equation:

$$k_{(E)}^{(n+1)} = \frac{f_{k(E)} \Delta t}{\rho^{(n+1)}} + k_{(E)}^{*(n+1)}. \quad (9)$$

The value of $k_{(E)}^{(n+1)}$ is used to update $k^{*(n+1)}$ which is used in the next time step.

This methodology is valid for the transport equations of k and ε when the information value is imposed at wall. The process is not valid for imposing an value of normal derivate property.

Boundary conditions for ε at walls

Use the dissipation rate coupled with the MDF method presents a significant difficulty, once there are different forms to consider its boundary condition. The first way is to impose a null derivative at the normal direction of the wall (Wilcox, 1994):

$$\frac{\partial \varepsilon}{\partial n} = 0. \quad (10)$$

Kinoshita *et al.* (2016) reported that the imposition of derivative using the MDF method is not possible, because the multiple forcing cannot be done. In other words, the process does not pass through a loop, which can compromise the convergence and, consequently, the obtained results. Thus, it is desirable to use a boundary condition of the Dirichlet type for a immersed boundary.

Besides Neumann boundary condition for ε , there are some authors that consider the Dirichlet boundary condition for ε at a wall, as shown by Wilcox (1994):

$$\varepsilon = \nu \frac{\partial^2 k}{\partial n^2}, \quad (11)$$

where ν is the kinematic viscosity of the fluid and n is the normal direction of the wall. There is still a way presented by Wilcox (1994), which is

$$\varepsilon = \frac{C_\mu^{3/4} k_P^{3/2}}{\kappa \delta_P}, \quad (12)$$

where $C_\mu = 0.09$ for the standard $k - \varepsilon$ model, k_P is the turbulent kinetic energy at the nearest point of the computational domain, $\kappa = 0.41$ and δ_P is the distance between the wall and the nearest point.

There are some other works consider the Dirichlet boundary condition for ε equals to zero:

$$\varepsilon = 0. \quad (13)$$

However, this boundary condition (Eq. 13) is not physically consistent in some problems, like the plane channel.

The methodology is equivalent using the Eqs. 11, 12 and 13 changing just the value of $k_{(L)}^{(n+1)}$ at Eq. 8.

COMPUTATIONAL SIMULATIONS

The proposed methodology was implemented in a in-house code developed at Fluid Mechanics Laboratory (MFLab), located in Federal University of Uberlandia (UFU), the MFSim code.

The MFSim is based in an adaptive block-structured regular and cartesian mesh which reduces the computational cost. Using this code, it is possible to simulate fluid-structure, multi-phase, reactive and turbulent flows with Large Eddy Simulation (LES) and URANS considering 3D domains and parallel processing (Neto *et al.*, 2019; Melo *et al.*, 2018; Denner *et al.*, 2014; Gasche *et al.*, 2012).

The MFSim has some temporal and advective discretization schemes and the possibility of using the SIMPLE method or fractional-step method for the pressure-velocity coupling.

Plane Channel

The first case simulated is a plane channel using periodic conditions in the stream-wise and span-wise directions and symmetry in the center of the channel. For the stream-wise direction a dynamic pressure gradient was used. This choice is justified by the possibility of perform simulations with and without the immersed boundary. The computational domain have $0.1 \times 0.0125 \times 0.01 \text{ m}^3$ and it was discretized in a hexahedral uniform grid. It was used $y^+ \approx 8$

and $y^+ \approx 4$ in the simulations. The Reynolds number (Re) of the flow is 13,750 which is the same one simulated by Mansour *et al.* (1988).

The Reynolds number and the wall coordinate y^+ are given by:

$$Re = \frac{\bar{u} \cdot (H/2)}{\nu}, \quad (14)$$

and

$$y^+ = \frac{u_\tau y}{\nu}, \quad (15)$$

where

$$u_\tau = \sqrt{\nu \left(\frac{\partial u}{\partial y} \right)_{wall}}. \quad (16)$$

After choosing the case, four simulations without the immersed boundary were performed and the only difference between them was the expression used for the boundary condition at the wall for ε (Eqs. 10, 11, 12 and 13). Considering the immersed boundary, only one simulation was performed for each mesh, in which was applied the value of Eq. 12 for ε at the wall. The final time of simulation is 0.35 s.

Flow Around a Cylinder

In order to observe the methodology in non-cartesian domains a second case were performed: the flow around a cylinder with $Re = 200\,000$, based on cylinder diameter.

At the bottom and top walls, the Neumann condition for velocities was applied. At the inlet, the Dirichlet condition was used and at the outlet, an advective condition was considered, both for velocities. In the span-wise direction, periodic condition was used for all properties.

The computational domain has $60D \times 40D \times 2.5D \text{ m}^3$. The cylinder is fixed in $x = 20D$ and $y = 20D$, with the origin of the domain at zero.

These simulations were performed with an adaptative mesh composed by five levels. The coarse level is a hexahedral uniform grid composed by 24.576 volumes. The finest level covers dynamically the immersed boundary and regions with high vorticity. For the simulations, a cylinder with $D = 0.1 \text{ m}$ and a flow with $U_\infty = 1 \text{ m/s}$ were considered.

Two simulations were performed and the drag coefficient obtained in both was compared with compared with experimental data. In the first simulation Eq. 13 was imposed in the immersed boundary. In the second case, Eq. 12 was forced in the immersed boundary.

All simulations were performed forcing $k = 0$ at the walls with the MDF method.

RESULTS AND DISCUSSION

Plane Channel

Through simulations without the immersed boundary, it was possible to verify that the k and velocity fields did not show any changes due to the different boundary conditions for ε . Even for the ε , it was noticed the same behavior for the interior of the channel. Fig. 1 shows this behavior for the velocity field. Given these results and based

on the arguments presented throughout the methodology, it was decided to perform only one simulation using immersed boundary.

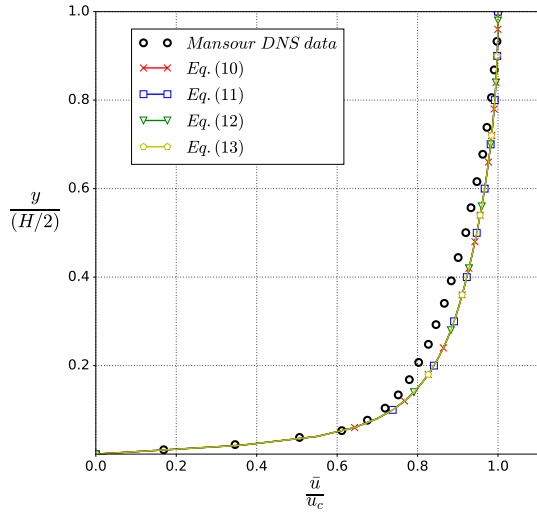


Figure 1. Normalized velocity profile obtained by simulations without immersed boundary using different boundary conditions for ε .

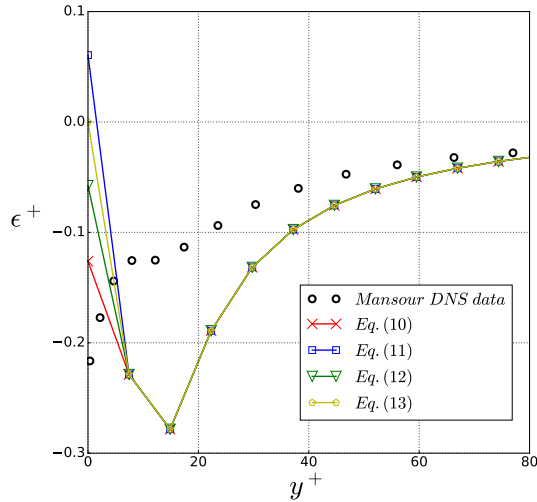


Figure 2. Normalized dissipation rate profile obtained by simulations without immersed boundary using different boundary conditions for ε .

The profiles obtained for k , ε and for the velocities field u and u_τ were compared with results from Direct Numerical Simulation (DNS) obtained by Moser *et al.* (1999).

Comparing the results, it was possible to observe a reasonable agreement between the simulation results with immersed boundary and without immersed boundary and the DNS results for the velocity field as shown in Fig. 3.

In the Fig. 4 it is possible to observe that the agreement between the MFSim simulation results and DNS data improves as the value of y^+ decreases. Furthermore, the results without immersed boundary are better than the results

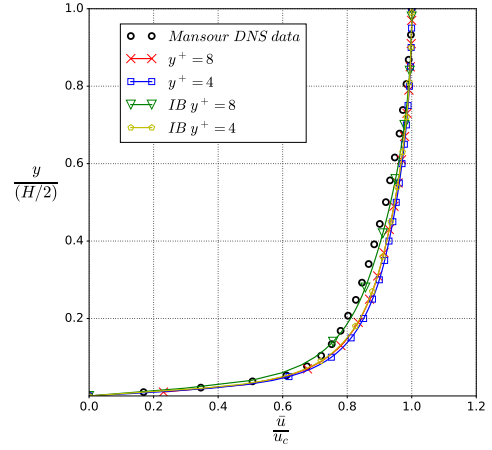


Figure 3. Non-dimensional mean velocity profile for the plane channel with $Re = 13750$.

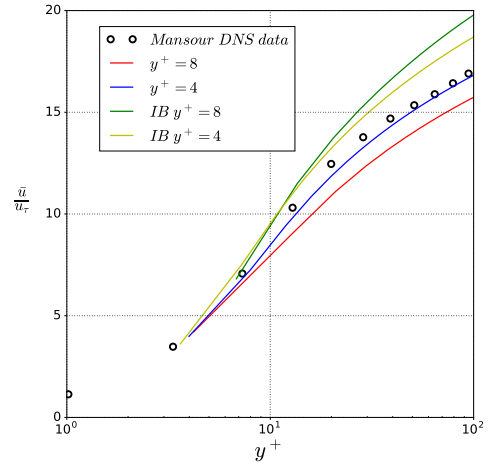


Figure 4. Non-dimensional velocity profile in wall coordinates for a plane channel with $Re = 13750$.

with immersed boundary, evidencing that the MDF have an intrinsic error.

The Fig. 5 show a non-dimensional profile of kinetic turbulent energy and the Fig. 6 shown a non-dimensional profile of dissipation rate, given by:

$$\varepsilon^+ = -\frac{\nu \varepsilon}{u_\tau^4}. \quad (17)$$

Second order moments, like k and ε have harder prediction than first order moments, like velocity. The results for k and ε with immersed boundary are worse than the results without immersed boundary.

The Multi-Direct Forcing is not the best method for boundary layer predictions because it involves many interpolations. The method and order of interpolations can change the results, mainly close to the wall. The MFSim have four types of interpolation function but in the simulations of the present work, only the hat interpolation was used because it presents the lowest computational cost.

Flow Around a Cylinder

The velocity field in x-direction is show in the Fig. 7 at $t^* = \frac{t U_\infty}{D} \approx 95$. It can be observe that the domain bound-

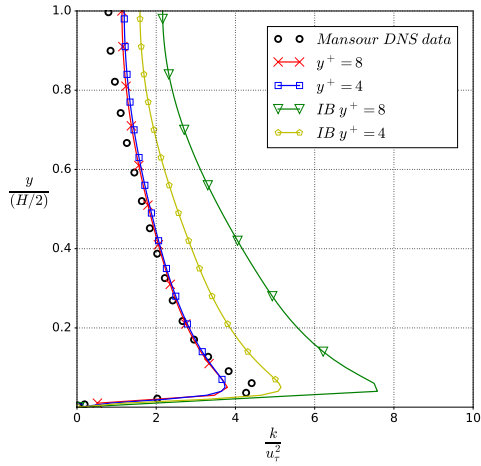


Figure 5. Non-dimensional profile of kinetic turbulent energy (k) for the plane channel with $Re = 13\,750$.

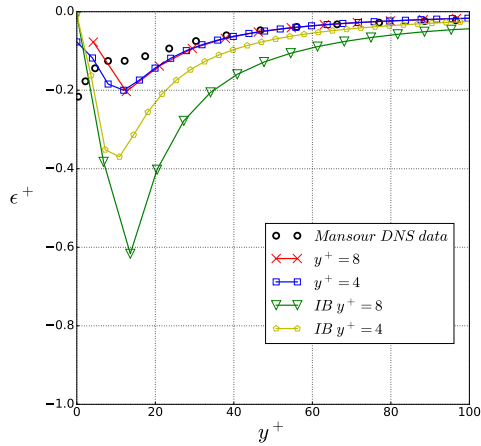


Figure 6. Non-dimensional profile of dissipation rate (ϵ) for the plane channel with $Re = 13\,750$.

aries are sufficiently far of the cylinder.

An interesting possibility of MFSim code is the dynamic adaptative mesh. Using dynamic adaptative mesh it is possible to cover a specific region of the domain with a fine grid. The regions with fine mesh can be defined by high gradients of informations or by the presence of immersed boundaries, for example.

In the simulations of the external flow around a cylinder a dynamic adaptative mesh was used based in immersed boundary and vorticity. The Fig. 8 shows the mesh in a region close to the cylinder at the same time of the flow field shown in Fig. 7.

Covering the domain only with the fine grid is expensive and covering the domain only with coarse grid leads to poor results. The most important parts of the flow are the wall of cylinder and regions with high vorticity.

Schlichting *et al.* (1974) presents drag coefficient according to the Re number for the flow around a smooth cylinder. For $Re = 2 \times 10^5$, the drag coefficient is approximately 1.18 ($C_D = 1.18$). Bearman (1969) found a drag coefficient of $C_D = 1.14$ in his experimental work for $Re = 2 \times 10^5$.

In Tab. 1, the results for drag coefficient are presented for the simulations with MFSim, and also the relative error between these results and the value found in the work of

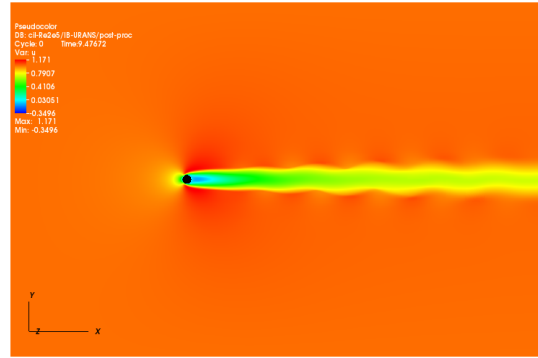


Figure 7. x -Velocity field at $t^* \approx 95$.

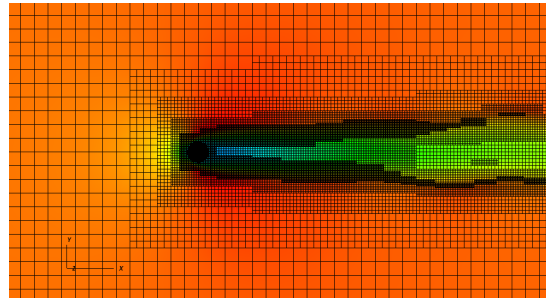


Figure 8. Detail of Fig. 7 for show the dynamic mesh with five levels.

Table 1. Drag coefficient for the flow around a cylinder with $Re = 2 \times 10^5$.

	C_D	Error (%)
Bearman (1969)	1.14	-
IB Eq. 13	1.225	7.46
IB Eq. 12	1.196	4.91

Bearman (1969).

The error using $\epsilon = 0$ in the wall is 7.46 %. It is a non-physical condition for many flows but it is correct in cases like an internal flow in a circular pipe (Laufer, 1954). Using the wall law derivative condition, given by Eq. 12, the error is 4.91 %. This is a physical condition for ϵ in walls.

In terms of computational cost per iteration, the two simulations are very close but the transient time for the simulation using Eq. 12 is bigger than using Eq. 13. The difference is about $60t^*$.

CONCLUSION

The simulations show that the methodology presents good results for a simple case: the plane channel. The obtained profiles had a concordance with DNS results and with URANS simulations without immersed boundary in MFSim. The MDF is a ship method for immersed boundary simulations and its objective is cost-benefit, non high accuracy.

The flow around cylinder shows that the methodology have a good behavior in simulations with non-cartesian geometries and coarse meshes. The values obtained for drag

coefficient are close with experimental result.

It can be concluded that the Multi-Direct Forcing with $k-\epsilon$ is a good alternative for simulations involving flow with immersed boundaries. This has a good performance in fine and coarse grids using together with the two-layer enhanced wall treatment.

More investigations with this methodology is being carried out to observe the behavior in many types of flows and to improve the developments.

REFERENCES

- Bearman, PW 1969 On vortex shedding from a circular cylinder in the critical Reynolds number regime. *Journal of Fluid Mechanics* **37** (3), 577–585.
- Denner, Fabian, van der Heul, Duncan R, Oud, Guido T, Villar, Millena M, da Silveira Neto, Aristeu & van Wachem, Berend GM 2014 Comparative study of mass-conserving interface capturing frameworks for two-phase flows with surface tension. *International Journal of Multiphase Flow* **61**, 37–47.
- Gasche, José Luiz, Barbi, Franco & Villar, Millena Martins 2012 An efficient immersed boundary method for solving the unsteady flow through actual geometries of reed valves.
- Kinoshita, Denise, Martínez Padilla, Elie Luis, da Silveira Neto, Aristeu, Pamplona Mariano, Felipe & Serfaty, Ricardo 2016 Fourier pseudospectral method for nonperiodical problems: A general immersed boundary method for three types of thermal boundary conditions. *Numerical Heat Transfer, Part B: Fundamentals* **70** (6), 537–558.
- Laufer, John 1954 The structure of turbulence in fully developed pipe flow.
- Launder, B. E. & Spalding, D. B. 1972 *Lectures in Mathematical Models of Turbulence*. Academic Press.
- Mansour, N Nd, Kim, John & Moin, Parviz 1988 Reynolds-stress and dissipation-rate budgets in a turbulent channel flow. *Journal of Fluid Mechanics* **194**, 15–44.
- Melo, RRS, Kinoshita, Denise, Villar, MM, Serfaty, R & Silveira-Neto, Aristeu 2018 Simulation of thermal transfer using the immersed boundary method and adaptive mesh. In *ICHMT DIGITAL LIBRARY ONLINE*. Begel House Inc.
- Moser, Robert D, Kim, John & Mansour, Nagi N 1999 Direct numerical simulation of turbulent channel flow up to $Re = 590$. *Physics of fluids* **11** (4), 943–945.
- Neto, H Ribeiro, Cavalini, A, Vedovoto, JM, Neto, A Silveira & Rade, DA 2019 Influence of seabed proximity on the vibration responses of a pipeline accounting for fluid-structure interaction. *Mechanical Systems and Signal Processing* **114**, 224–238.
- Schlichting, Hermann *et al.* 1974 *Boundary-layer theory*. Springer.
- Wang, Zeli, Fan, Jianren & Luo, Kun 2008 Combined multi-direct forcing and immersed boundary method for simulating flows with moving particles. *International Journal of Multiphase Flow* **34** (3), 283–302.
- Wilcox, David C. 1994 *Turbulence modeling for CFD*. DCW Industries Inc.